Cloud Publications
International Journal of Advanced Earth Science and Engineering
2017, Volume 6, Issue 1, pp. 538-547
ISSN: 2320 – 3609, Crossref: 10.23953/cloud.ijaese.276

Case Study

Stress Field Delineation using Well Log Data – A Case Study

Rakhi Arvind Pandey

Western offshore basin ONGC, Mumbai, Maharashtra, India

Publication Date: 10 June 2017

DOI: https://doi.org/10.23953/cloud.ijaese.276

Abstract The essentiality of stress field delineation in the subsurface arises in several contexts like well planning and monitoring to ensure safe drilling of a borehole. Work reported here concerns with methodology developed for delineating stress fields in rock strata using log data which includes crossed dipole and monopole acoustic data acquired in boreholes. Orientation of the principal stresses in the horizontal plane has been arrived at by computing relative azimuth of maximum and minimum stress directions with respect to a designated dipole transmitter's axial orientation. Static Poisson Ratio and Static Young's modulus have been computed using customized relationships with due care has been taken to factor-in fluid effects where compressible fluids are known to present within pore space of the rock. Stresses magnitudes and UCS model have been subjected to a validity check through prediction versus actual of presence / absence of breakouts (the latter from image data evidence) and the match is very good.
Keywords *LOT; maximum horizontal stress; minimum horizontal stress; XLOT*

1. Introduction

Delineation of local stress field and its relationship between regional stress fields, gives the all-important depth-wise behavior of magnitude as well as orientation of the principal stresses. The distinguishing features of the work flows are modeling azimuthally anisotropic principal stresses in horizontal plane using fast shear and slow shear slowness and a realistic model of residual strains (due to residual tectonic stresses). LOT/XLOT data used as calibration, and a robust validation scheme wherein borehole failure or absence thereof is predicted from model and cross checking for validity with electric images data. Borehole images and drilling observations have been noted as fully corroborating model based predictions and Static Young's Modulus, PR,UCS and Friction angle are validated by laboratory estimation based on cores cut in stratigraphic and lithological rock in a well currently under drilling and not necessarily a part of the case study reported.

2. Area of Study

The work flows have been developed for exploration areas off Kutch-Saurashtra coast India [1].The case study presented involves 2 wells and well sections pertaining to tertiary as well as pre-tertiary have been made a part of the case study. Two wells have been analyzed; general information of the same is given below

Table 1: *General information of studied wells* [2][3]

	Well 1	Well 2
Target depth	4250m	2030m
Drilled Depth	4250m	2030m
Water Depth	12.80m	27.11m

3. Methodology Adopted

Input data sets include resistivity, nuclear, gamma ray logs and formation tester pressures, electrical Images and complemented by LOT and XLOT data acquired during the drilling. Monopole excitation derived acoustic wave forms inclusive of Stoneley mode, multiplexed crossed dipole excitation (from crossed dipole transmitters) derived flexural wave trains. From the advanced acoustic data sets mentioned above compressional slowness, fast and slow shear slowness and Stoneley mode slowness of the formation is derived.

In the current study it has been assumed that reservoir rock has isotropic elastic properties in unstressed state, which is also supported by image data. Thus it is assumed that anisotropy in rock mechanical properties arises only due to stress anisotropy. Vp/Vs have been computed as ratio of shear wave slowness to compressional wave slowness. Dynamic elastic moduli has been computed as

$PR_{Dyn} = (Vp/Vs)^2 – 0.5)/ (Vp/Vs)^2 – 1.0)$
$G = \rho_b * Vs^2$
$E_{Dyn} = 2G (1+ PR_{Dyn})$

Where, PR_{Dyn}-Dynamic Poisson's ratio, G-Shear Modulus, E_{Dyn}- Dynamic Young's modulus. Vp-Compressional velocity of formation (computed as reciprocal of compressional slowness). Vs -Shear velocity of formation (computed as reciprocal of shear slowness), and ρ_b-formation bulk density. Stress Field delineation relies on static moduli and therefore it is necessary to compute static moduli of elasticity starting from the dynamic moduli data. The computation is discussed below.

A) Computation of PR_{Static} (The symbol 'v' will henceforth denote PR_{Static} in this paper)

From a theoretical standpoint the relationship between static and dynamic Poisson Ratio values has to depend on two factors firstly the ratio of population of high aspect ratio pores to that of low aspect ratio pores, abundance of open cracks and confining pressure (more the confining pressure less the open cracks left). These are difficult to model into an effective medium theory when the data sets comprise well log data. Therefore a different approach has been followed in the current case study. Survey of literature brings home the fact that the most productive form of relation between Dynamic and static PR is of the linear form

$PR_{Static} (v) = k^* PR_{Dyn}$

B) Computation of Static Young's Modulus (E_{Static})

For our present study we have adopted a linear relationship between Static Young's Modulus (E_{Static}) and Dynamic Young's Modulus (E_{Dyn}). The relationship we have used is

$E_{Static} = 0.809^* E_{Dyn}$.

This form of the relationship and the subsequent UCS models based on E_{Static} have been seen to be well validated by match between behavior of formation face exposed in the different well sections from the perspective of predicted presence / absence of mechanical failure of formation at and near borehole and actual condition as confirmed from borehole images.

C) Modeling of UCS and Tensile strength of Rocks

For modeling UCS we have used a power law type of relationship between UCS and E_{Static} of the form

$$UCS = A^* (E_{Static})^B$$

Value of modeled UCS is constrained by presence or absence of shear failure of formation at and near borehole wall. We have arrived at the following values for A and B where we have seen a consistency lithology wise and whether the rock is an outcome of a tertiary or pre-tertiary deposition. The sections studied in our current work comprise tertiary as well as younger depositions. The values of A B used lithology which we have used to model UCS have been found to be consistent lithology and age wise. These values are given in Table 2.

Table 2: *Constant used in UCS calculation*

Age	Lithology	A	B
Tertiary	Shale	3.3-3.7	0.33-0.37
	Siltstone	3.5	0.35
	Sandstone	2.5	0.25
	Limestone	3.5	0.35
Pre-Tertiary	Shale	4.5	0.45
	Siltstone	4.1	0.35
	Sandstone	4.1	0.35
	*Limestone	-	-
*Not encountered in studied wells			

In conformance with the relationship assumed between UCS and Tensile strength of rocks a linear relation has been assumed as relating Tensile Strength of rock to UCS. The relation used in the current work is

$$T = UCS/11.1$$

Where, T-Tensile Strength of rock and UCS its Unconfined Compressive strength.

D) Computation of shear moduli of elasticity relevant to shear stresses and shear strains in the respective principal planes

Considering, a co-ordinate system with X axis along the maximum horizontal stress direction. Y axis along the minimum horizontal stress direction and z axis along the vertical direction. C44 C55 C66 respectively corresponds to shear moduli applicable for shear stresses and strains in the principal planes yz xz and xy respectively. If ρb is the formation density C44 C55 and C66 are computed as

$$C44 = \rho b \, Vsslow^2$$
$$C55 = \rho b \, Vsfast^2$$
$$C66 = \rho mud / [(DTmud)^2 - (DTstoneley)^2]$$

E) Modeling of Friction Angle (φ)

Friction angle φ for grain supported rock facies has been computed using the Weingarten and Perkins (1999) correlation [6]

φ = 57.5-105ψ where φ is expressed in Degrees and ψ sands for porosity in units of volume fraction.
Friction angle φ for mud supported rock facies has been computed using the correlation given by Lal (1992) [4]

φ = sin-1((Vp-1000)/ (VP+1000))
where φ is in radians and Vp is compressional velocity for the rock in units of m/sec.

F) Analysis of LOT / XLOT data

Out of the well sections studied, LOT data exists for all sections. Additionally XLOT data exists for two sections one in well NAA-1. XLOT data available for well NAA-1 comprises pump pressure volume pumped and time elapsed data The objective of this analysis had been estimation of magnitude of minimum horizontal stress, and also to confirm that only a single fracture was initiated.

G) Analysis of XLOT data for estimating minimum horizontal stress magnitude at XLOT depth

Pump pressure has been plotted on y axis against volume of mud pumped on x axis. The value of pump pressure PLOP at which first deviation from linear relation between pump pressure and volume pumped, occurs has been considered as surface pressure corresponding to leak off pressure in the subsurface. Leak off pressure has been considered as an estimate of minimum horizontal stress magnitude where only LOT data is available. Leak-Off Pressure has been computed as PLOP + pressure due to hydrostatic column in the borehole from surface down to the LOT depth.

H) Estimation of pore pressure (Pp)

Wells studied have a rich data set of formation tester pressures. The data density is enough to have reliable trends of pore pressure vs depth. Formation pressure vs depth trends indicate normal pressure regime with maximum increase not exceeding hydrostatic plus 10%. Hence no regular pore pressure prediction work flow was necessitated and none attempted.

I) Computation of magnitudes of principal vertical stress

Vertical stress σv has been computed by adding the stress due to water column and stress due to sediment weight. Density logs are not available up to the mud line. Mud line sediment density has been assumed from area knowledge and where soil coring penetration data is available, from an estimate of likely mud line sediment density therefrom. A linear increase of sediment density from mud line to the shallowest depth of available density log data has been assumed. Such an assumption is not unreasonable since shallowest density log depth would involve around 150m of sediment column above this depth level, which column would correspond to the upper half of a hypothetical column from mud line to a depth where the sediment porosity would go below the critical porosity value for the shallow sediments encountered. After bringing the available density log depth thus up to mud line level this sediment density versus depth function has been integrated with respect to depth to obtain sediment load derived vertical stress for any depth level. The stress due to the weight of water column above mud line has been added to get the vertical stress.

J) Computation of magnitudes of principal stresses in the horizontal plane

If σv, σH, σh stand for the vertical maximum horizontal and minimum horizontal principal stress magnitudes respectively then these are related to C44 C55 C66 as

(C44 - C66) / (C55 - C66) = (σv - σH)/(σv - σh) [5]

Therefore by evaluating the LHS we evaluate the RHS which we denote as 'ξ'

Then σH = ξ* σh + 1- ξ* σv

At LOT / XLOT depth level the value of σh is estimated as discussed in the foregoing and σH computed as from above. The value of σH / σh is computed at LOT / XLOT depth level and denoted as 'λ'

Next, horizontal stress magnitude in absence of residual tectonic stresses is computed as

σ0 = (v/(1- v))*(σv – Pp) + Pp where Pp is pore pressure and v is static Poisson Ratio.

It is assumed that deviation of magnitude of actual principal stresses in horizontal plane is expression of residual tectonic stresses. Residual tectonic stresses would result in anisotropic strain field in horizontal plane. If εH and εh respectively stand for magnitude of additional strain along maximum horizontal stress direction and minimum horizontal stress direction respectively then the following relations apply

$\sigma h = \sigma 0 + (Estatic/(1- v^2))* \varepsilon h + (Estatic* v /(1- v^2))* \varepsilon H$
$\sigma H = \sigma 0 + (Estatic* v /(1- v^2))* \varepsilon h + (Estatic /(1- v^2))* \varepsilon H$

From LOT/ XLOT data analysis described in the foregoing magnitude of σh at LOT / XLOT depth is computed. Subsequently σH magnitude at LOT / XLOT depth level is also computed as described in the foregoing.

The ratio (σH / σh) is designated here as 'λ' and its value is computed for LOT / XLOT depth level as described above. We have, in light of equations for σh and σH above and equation

σH = ξ* σh + 1- ξ* σv
εh/ εH = {(σh – v* σH) – (1- v)* σ0} / {(σH – v* σh) – (1- v)* σ0}

The ratio (εh/ εH) is designated here as 'μ' and its value is computed for LOT / XLOT depth level as described above.

In the course of our work we have noted integrating area knowledge that LOT / XLOT depths are shallow level depths of respective well sections (within which they occur) that share common tectonic history. Hence it is reasonable to assume that these sections respectively share their λ and μ values with the depth levels where LOT /XLOT had been conducted. Therefore it has been assumed that λ and μ values computed for LOT / XLOT depths are applicable for each level of the respective sections which the LOT / XLOT depth levels form part of. And therefore level by level evaluation of σh, σH as

σh = {σ0*(1- μ)*(1- λ)}/{1 - v*(λ - μ)- λ*μ}
σH = σh* λ

In some of the well sections studied it was noted by us that usable fast shear and slow shear data could not be derived. However we have noted that this data is available against correlated section in nearby wells. We have used the ξ parameter value for those sections to compute σH at LOT / XLOT depths in accordance with the relation

σH = ξ* σh + 1- ξ* σv and computed λ and μ in accordance with the computation above and thereby computed σh and σH level by level in accordance with the method shown above.

K) Computation of Orientation of the principal stresses in space

One of the principal stresses is oriented vertically. We set up a coordinate system in which z axis is taken as vertical, x axis taken along maximum horizontal stress direction and y axis is taken along minimum horizontal stress direction. Another coordinate system is also considered which has its z axis along the tool axis and hence the borehole axis, its x axis along the axis of the designated dipole transmitter, and which is also called the tool face and its y axis orthogonal to the above two axes. We denote this coordinates system as the x1y1z1 coordinates system. With the acoustic tool a directional triaxial package is also run which enables us to know the inclination of the tool axis with respect to the vertical and thus the angle between z and z1 axes, and the azimuth of x1 with respect to true north. Through a workflow called as four component rotation the azimuth of x1 with respect to x is computed using the in line and cross line dipole array receivers responses to crossed dipole transmitters excitation. Since azimuth of x1 with respect to true north is known the azimuth of x and therefore of y axes with respect to true north is now known. And thus the orientation of the principal horizontal stresses is known. Since the other principal axis is vertical the stress field is spatially delineated.

Since the magnitude of principal stresses is also by now computed as discussed in detail in the foregoing, the stress field stands completely delineated in magnitude as well as directionally.

4. Validation of Results

Using model data of the rock mechanical properties, minimum mud weight predicted as necessary to be exceeded in order to avoid bore hole breakout (denoted as Pmbrout) and the maximum mud weight threshold (Pmfrac) which when exceeded by effective circulation density (ECD) would result in tensile failure of the formation at the bore hole wall, have been computed for all levels applying Mohr-Coulomb Failure Criteria.

Pmbrout and Pmfrac have been computed using the following relations

Pmbrout = [1/(Kp+1)]*{3*σH – σh – UCS + (Kp-1)*Pp} / {(D*1.422)/8.33)}
Where D is depth in meters, of the level for which Pmbrout is being computed, and Kp the Passive

Mohr-Coulomb Coefficient is given by
Kp = (1+sinφ)/ (1-sinφ), φ being friction angle.

All other variables and parameters on RHS are in units of psi. Pmbrout is computed in units of ppg).
Pmfrac = {3*σh–σH–Pp + T} / {(D*1.422)/8.33)}
Where D is depth in meters, of the level for which Pmfrac is being computed, and T is Tensile Strength of formation.

All variables other than D on RHS are in units of psi. Pmfrac is computed in units of ppg).

Pmbrout and Pmfrac are thus respectively the end points within which ECD has to be managed in order to ensure that neither shear failure nor tensile failure of formation would occur during drilling of the well (Figure 1). The accuracy and hence usefulness of the computed values of Pmbrout and Pmfrac against different depth levels has been checked, using FMI image data, FMI recorded in reservoir interval shows breakout from 2300- 2600m (Figure 2) and from the Figure 1, it is very much clear that mud weight is less than required mud weight (threshold mud weight) to overcome breakout. FMI images also show the direction of breakout i.e. minimum horizontal stress (as breakout always occur in this direction) and rose diagram of fast shear azimuth (Figure 3) shows the direction of maximum horizontal stress as NE which is orthogonal to minimum horizontal stress. Figure 2 (FMI Images) shows the azimuth of breakout NW-SE which is orthogonal to what Figure 3 shows (rose diagram) as fast shear azimuth which is direction of maximum horizontal stress. Since breakouts occur along direction of minimum horizontal stress, clearly images validate the fast shear azimuth obtained from advanced acoustic data processing. Thus model predictions on principal stress orientations are also validated. Similar validation is presented for well 2 where model does not predict formation mechanical failure at bore hole wall (Figure 5) which prediction is validated by images against the relevant interval (Figure 6).

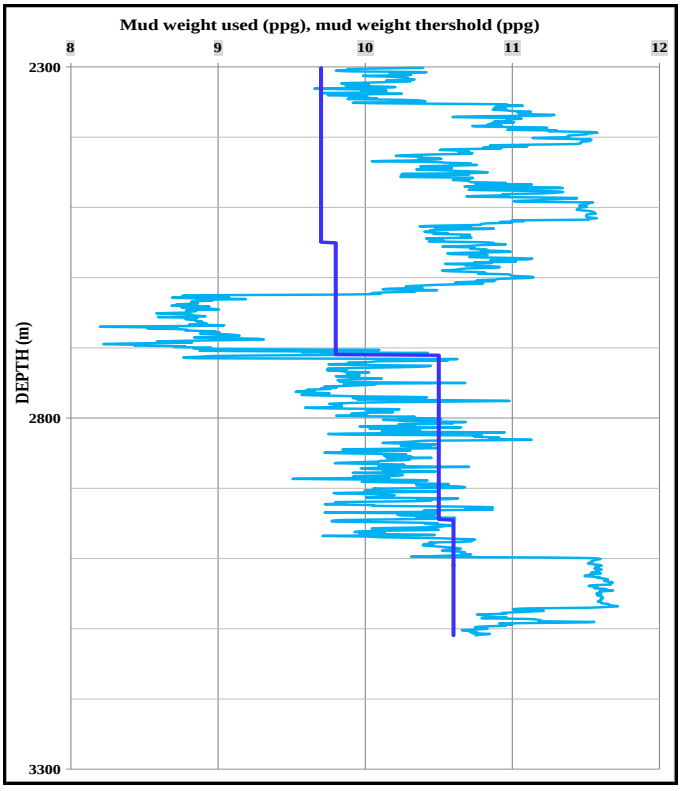

Figure 1: *Calculation of Pm brout vs mud weight used in well 1*

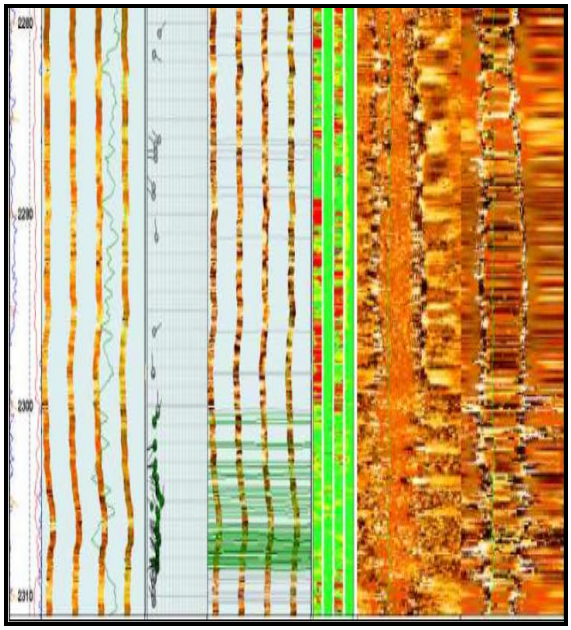

Figure 2: *FMI image encountered against the reservoir interval showing breakout in well 1*

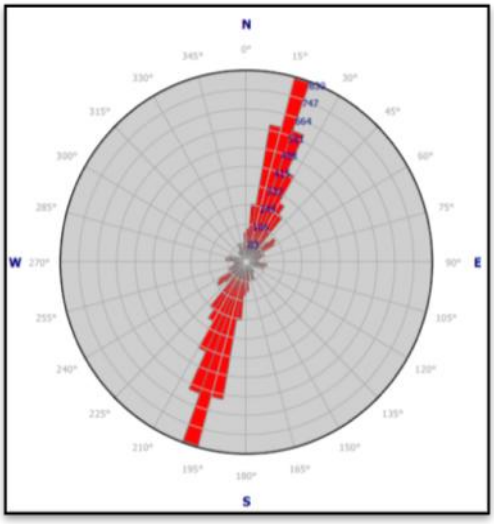

Figure 3: *Rose diagram of fast shear azimuth*

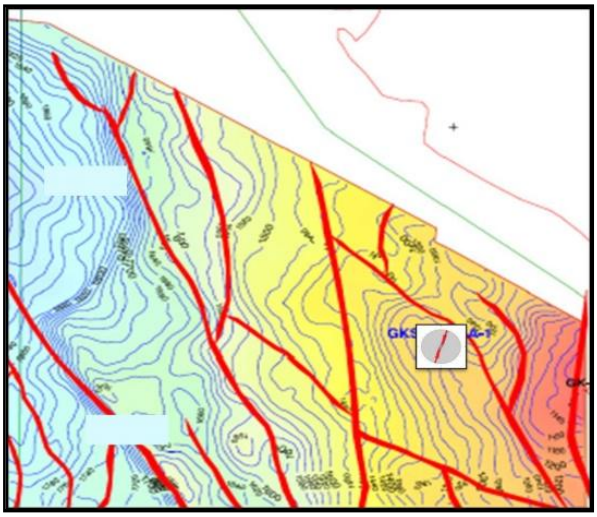

Figure 4: *Rose diagram of fast shear azimuth against the studied well plotted over Time Structure Map at the top of Bhuj formation (Age-Cretaceous)*

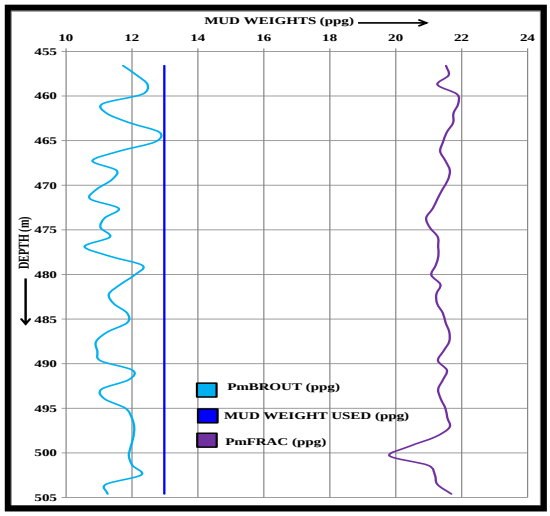

Figure 5: *Calculation of Pm brout vs mud weight used in well 2*

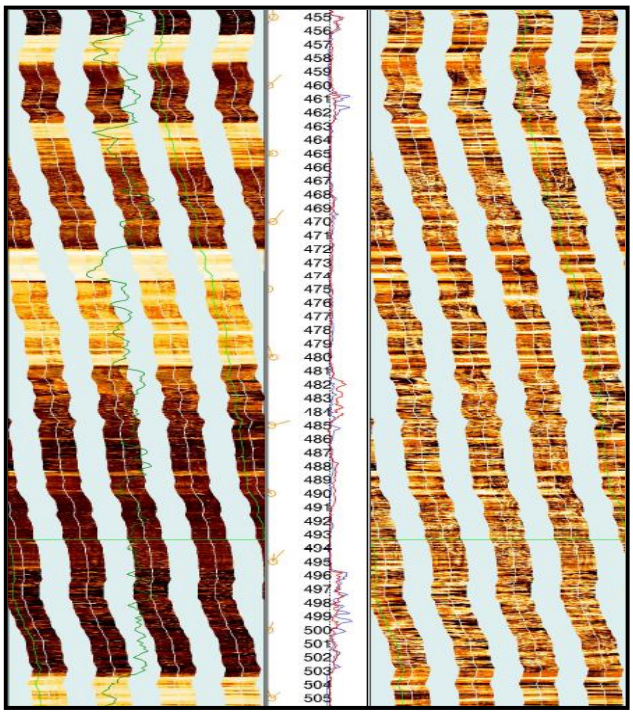

Figure 6: *FMI image encountered against the reservoir interval showing breakout in well 2*

5. Results and Discussion

σH, σh, σv and σ0 have been presented as plots against depth for different sections studied. The results bring out that the stress regime as today is normal stress regime. This indicates that even for the cases of inversion the deformability of the sediment layers coupled with subsequent tectonic history has led to normal stress regime to be the stress signature for the study area. Individual well wise maximum horizontal stress directions have been presented as rose plots which show that direction of maximum horizontal stress is NE SW dominantly in the area. Examination of the ratio (σH/σh) brings out that across different wells and different stratigraphic sections horizontal stress anisotropy is of a low degree. This is in line with the general geological understanding of the areas of studied. Regional Stress Distribution has been superimposed on the same maps in order to show the degree of conformity or otherwise between the locally delineated stress field's spatial orientation vis-a-vis that of the regional field. It is noted that the degree of conformance is good.

6. Conclusions

A viable methodology for stress field delineation has been demonstrated which is based on robust modeling with in-built means of constraining model parameters and validation by images, drilling observations, well history and laboratory results. Strong LOT/XLOT data support crossed dipole acoustic data and low frequency monopole data for stoneley mode properties in addition to compressional slowness determination, formation tester data of sufficient data density and good quality images and conventional resistivity nuclear gamma suites are a necessary requirement for implementing the workflows demonstrated in this work.

References

[1] Zutshi, P.L., Sood, A., Mahapatra, P., Ramani, K.K.V., Dwivedi, A.K. and Srivastva, H.C.: Lithostratigraphy of Indian Petroleum Basins. Document V: Bombay offshore Basin. KDMIPE Dehradun. (1993)

[2] Well completion report of well-1 (actual name modified). Geological operation group ONGC, Mumbai. Unpublished report. (2014).

[3] Well completion report of well-2 (actual name modified). Geological operation group ONGC, Mumbai. Unpublished report. (2015).

[4] Lal, M.: Shale stability: drilling fluid interaction and shale strength. SPE Latin American and Caribbean Petroleum Engineering Conference held in Caracus, Venezuela. (1999)

[5] Sinha, K.B.: Recent advances in Borehole Sonic Technology. 7th International Conference & Exposition on Petroleum geophysics. 163 (2008)

[6] Weingarten, J.S., Perkins, T.K.: Prediction of sand production in gas wells: method and Gulf of Mexico case studies. Paper SPE 24797 Washington DC, 4/7 October. (1992)